

Supporting Information

Synthesis of Magnetic, Fluorescent, and Mesoporous Core-Shell –Structured Nanoparticles for Imaging, Targeting and Photodynamic Therapy**

Fang Wang^a, Xiaolan Chen^{*a}, Zengxia Zhao^a, Shaoheng Tang^a, Xiaoqing Huang^a,
Chenghong Lin^b, Congbo Cai^b, and Nanfeng Zheng^{*a}

^a State Key Laboratory for Physical Chemistry of Solid Surfaces and Department of Chemistry, Xiamen University, Xiamen 361005, China

E-mail: chenxl@xmu.edu.cn, nfzheng@xmu.edu.cn

^b Departments of Physics and Communications Engineering, Xiamen University, Xiamen 361005, China

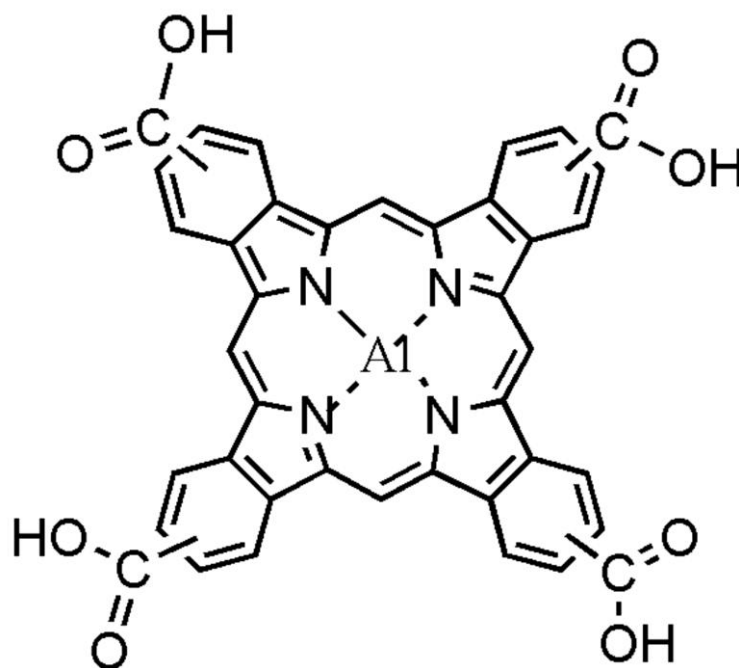


Figure S1. The structure of AlC₄Pc.

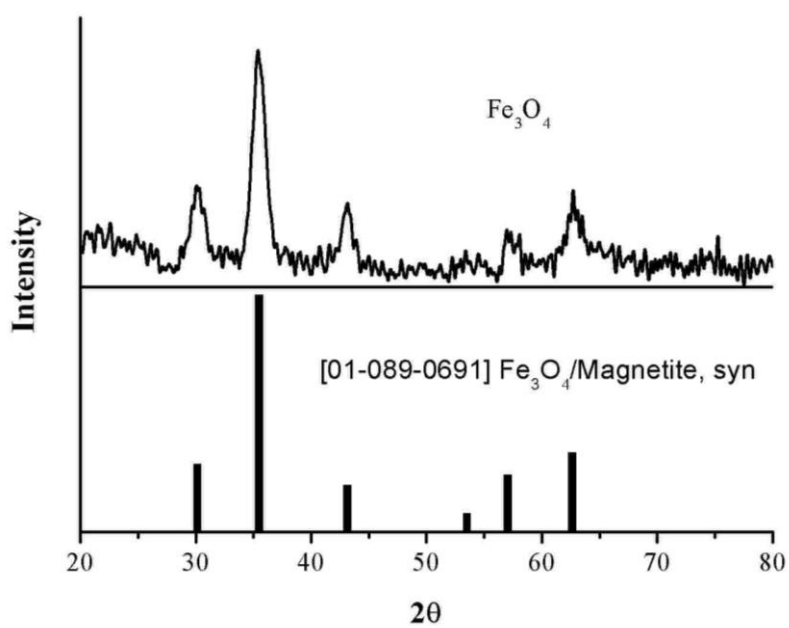


Figure S2. XRD pattern of Fe_3O_4 nanoparticles.

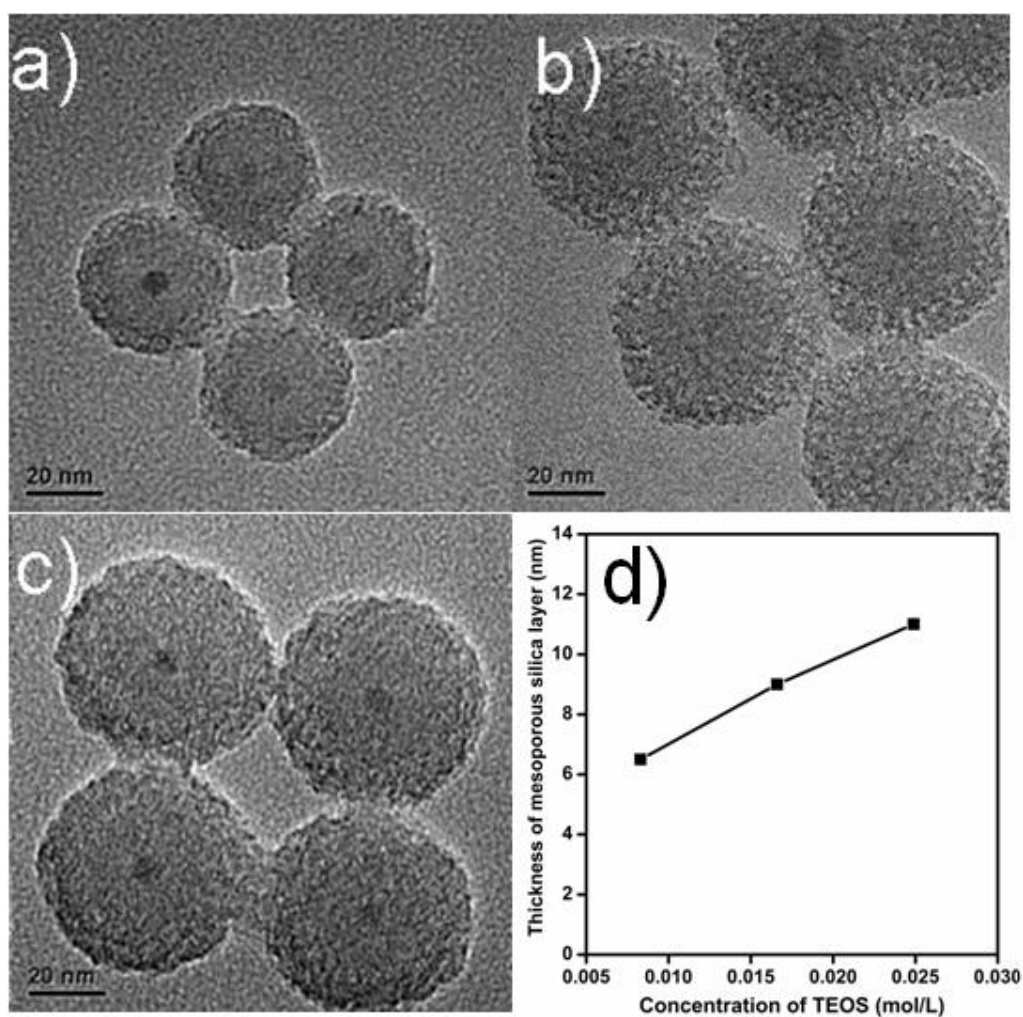


Figure S3. TEM images of Fe₃O₄@SiO₂(F)@meso-SiO₂(P) with different amounts of TEOS, a) 8.3×10^{-3} mol/L, b) 1.66×10^{-2} mol/L and c) 2.49×10^{-2} mol/L, respectively. d) Effect of TEOS concentration on the thickness of mesoporous silica layer at a fixed 8 h reaction time. The thickness of mesoporous SiO₂ layer from a) to c) is about 6.5 nm, 9 nm and 11 nm, respectively.

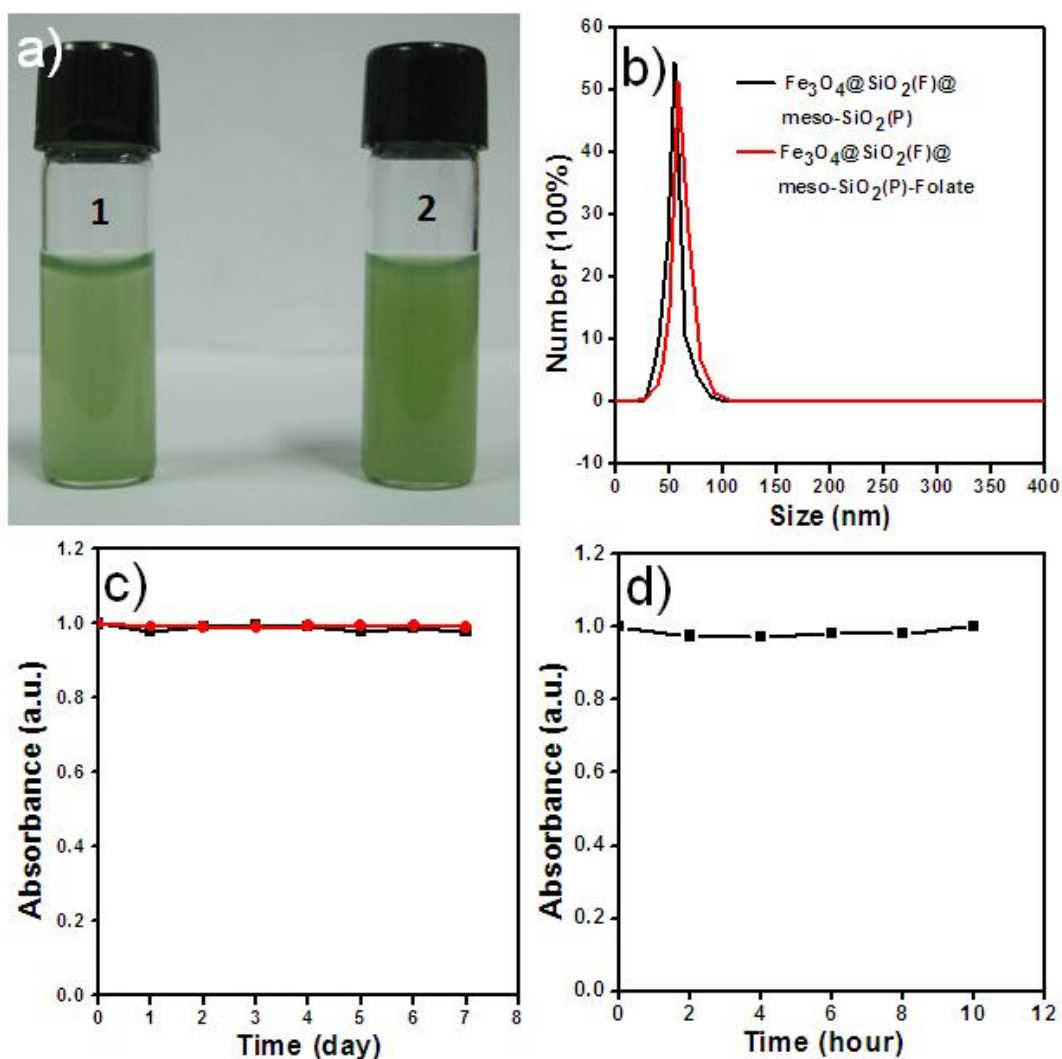


Figure S4. (a) Digital photographs of $\text{Fe}_3\text{O}_4@ \text{SiO}_2(\text{F})@ \text{meso-SiO}_2(\text{P})$ (1) and $\text{Fe}_3\text{O}_4@ \text{SiO}_2(\text{F})@ \text{meso-SiO}_2(\text{P})\text{-Folate}$ (2) nanoparticles dispersion in water. (b) DLS of $\text{Fe}_3\text{O}_4@ \text{SiO}_2(\text{F})@ \text{meso-SiO}_2(\text{P})$ and $\text{Fe}_3\text{O}_4@ \text{SiO}_2(\text{F})@ \text{meso-SiO}_2(\text{P})\text{-Folate}$ nanoparticles in water. The dispersion stability of $\text{Fe}_3\text{O}_4@ \text{SiO}_2(\text{F})@ \text{meso-SiO}_2(\text{P})$ or $\text{Fe}_3\text{O}_4@ \text{SiO}_2(\text{F})@ \text{meso-SiO}_2(\text{P})\text{-Folate}$ nanoparticles in water (red) and in PBS (black) for seven days respectively (c), and in cell medium for 10 h (d).

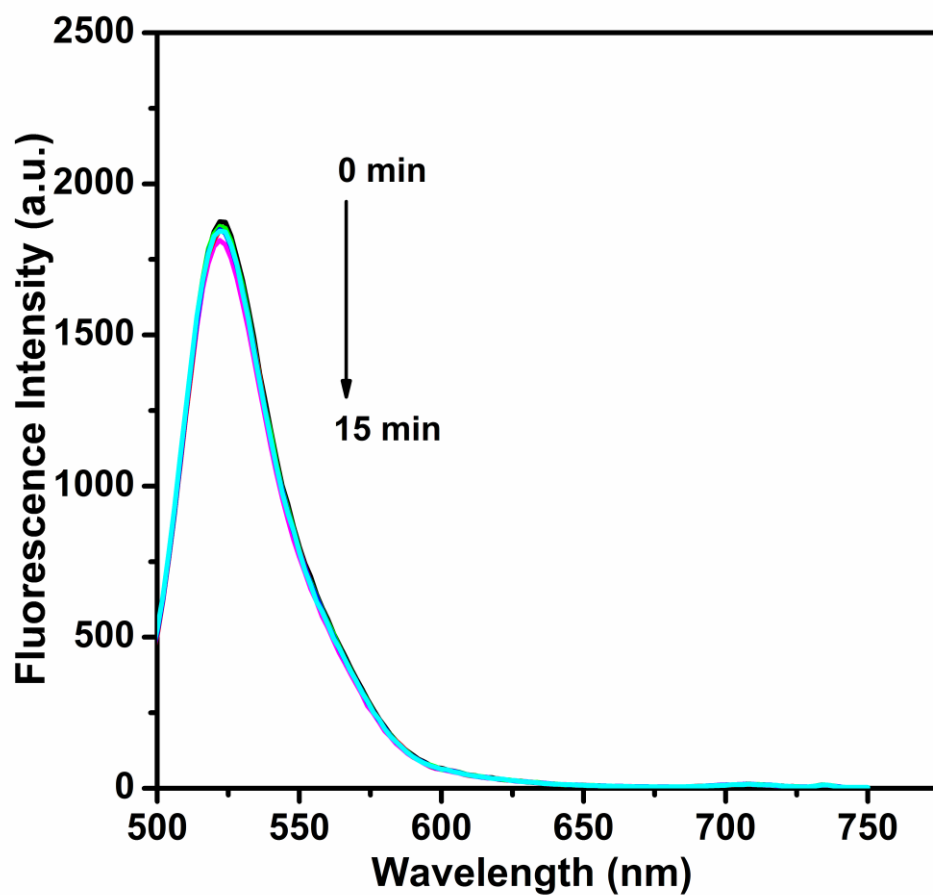


Figure S5. Fluorescence spectra of $\text{Fe}_3\text{O}_4@\text{SiO}_2(\text{F})@\text{meso-SiO}_2(\text{P})$ under 488 nm excitation after different periods of irradiation with a 660 nm laser beam.

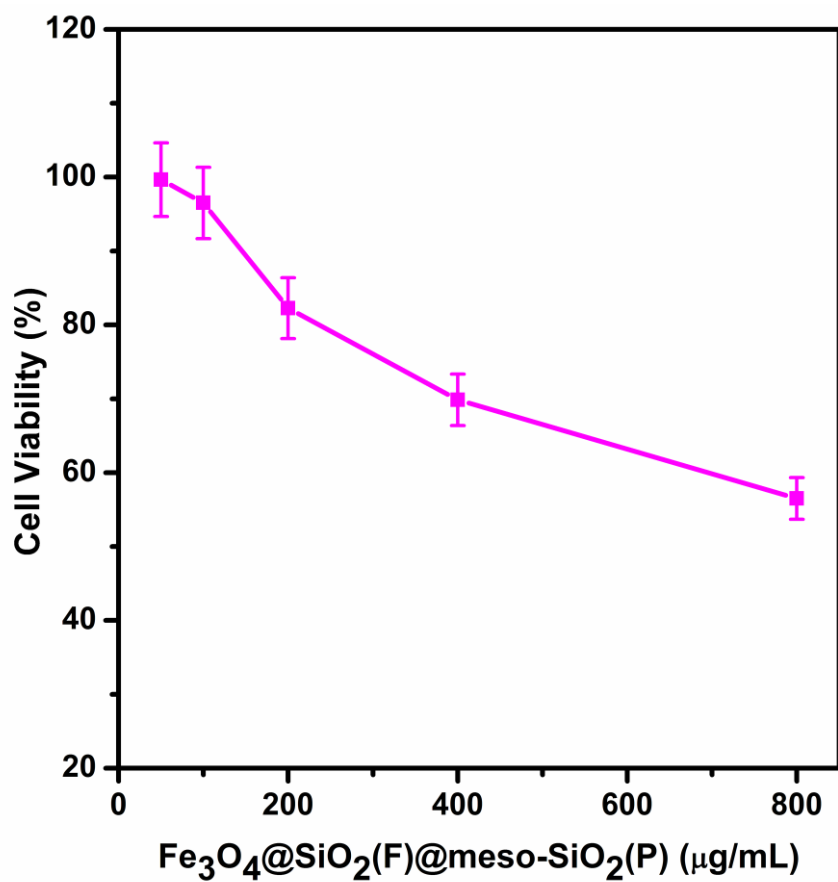


Figure S6. The viability of human hepatocyte cells incubated with Fe₃O₄@SiO₂(F)@meso-SiO₂(P) at different concentrations.

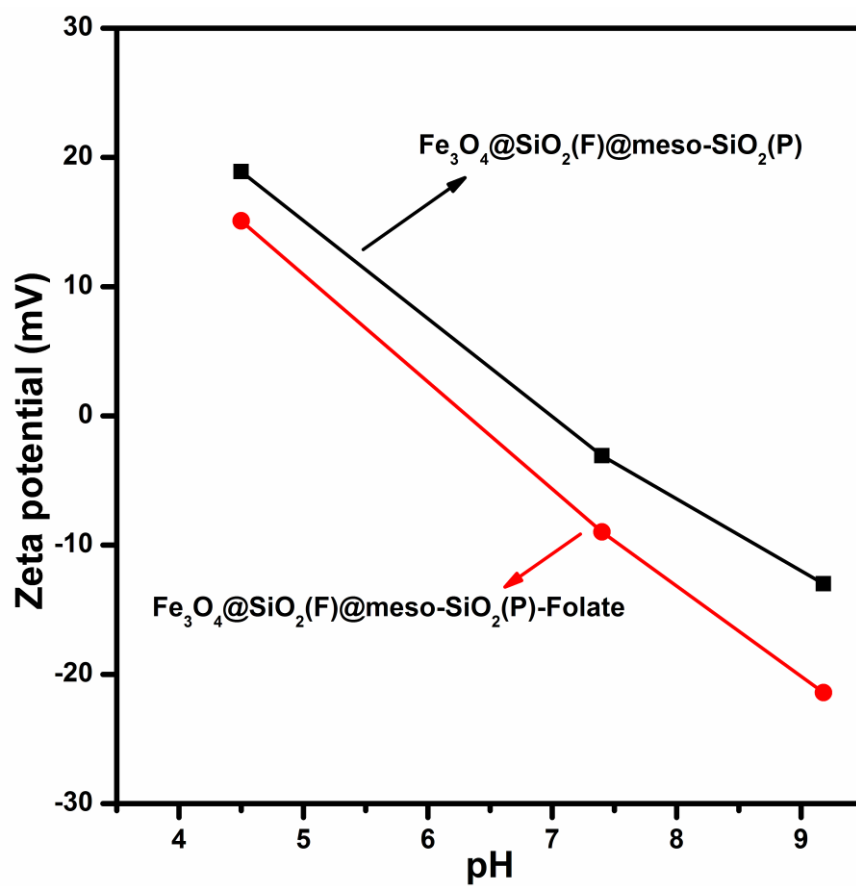


Figure S7. The zeta-potential of $\text{Fe}_3\text{O}_4@SiO_2(F)@meso-SiO_2(P)$ and $\text{Fe}_3\text{O}_4@SiO_2(F)@meso-SiO_2(P)\text{-Folate}$ nanoparticles at different pH.

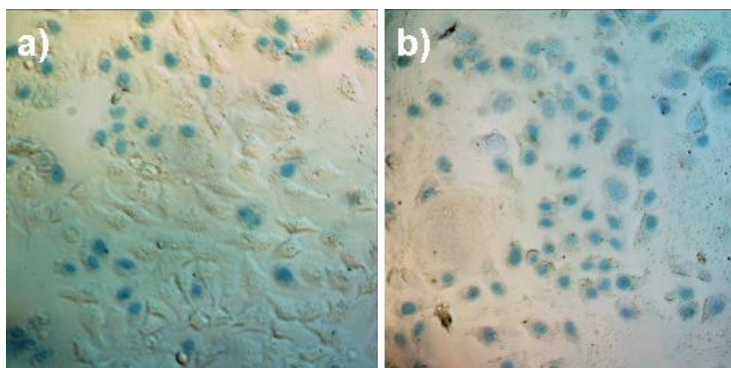


Figure S8. Optical imagings of HeLa cells stained with Trypan blue after different treatment: a) 100 $\mu\text{g/mL}$ $\text{Fe}_3\text{O}_4@\text{SiO}_2(\text{F})@\text{meso-SiO}_2(\text{P})$ and 10-min light exposure with 75 mW/cm^2 ; b) 100 $\mu\text{g/mL}$ $\text{Fe}_3\text{O}_4@\text{SiO}_2(\text{F})@\text{meso-SiO}_2(\text{P})\text{-Folate}$ and 10-min light exposure with 75 mW/cm^2 .

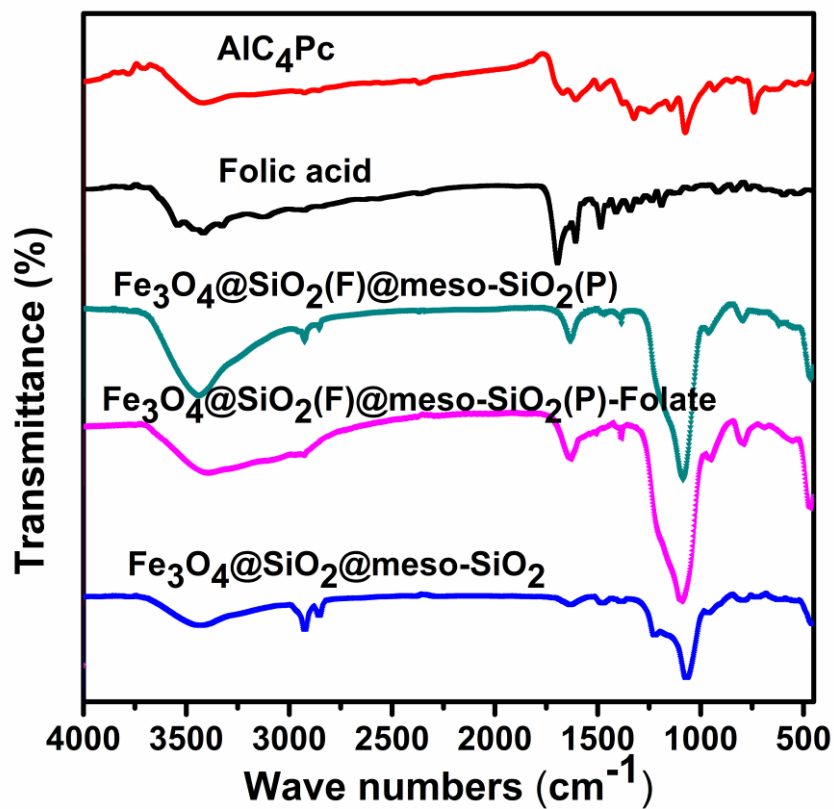


Figure S9. FT-IR spectra of Fe₃O₄@SiO₂(F)@meso-SiO₂(P) and Fe₃O₄@SiO₂(F)@meso-SiO₂(P)-Folate.